Electronic Supplementary Material (ESI) for New Journal of Chemistry.
This journal is © The Royal Society of Chemistry and the Centre National de la Recherche Scientifique 2022

Hexacoordinate high-spin Fe(III) complexes composed of pentadentate amino-type ligand and pseudohalido coligands

Cyril Rajnák, Romana Mičová, Zuzana Bielková, Ján Titiš, Milan Gembický, Franz Renz, Ondřej Malina, Erika Samoľová, Jana Nováčiková and Roman Boča

List of compounds

Free ligand L^{im}

Free ligand L^{am}

1 $[Fe(L^{am})(Cl)]$

2 $[Fe(L^{am})(NCSe)]$

3 $[Fe(L^{am})(NCS)]$

4 $[Fe(L^{am})(N_3)]$

5 $[Fe(L^{am})(NCO)]$

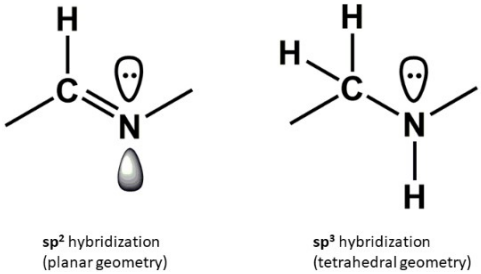

Figure S1. Two forms of hybridization: left – imine; right – in secondary amine.

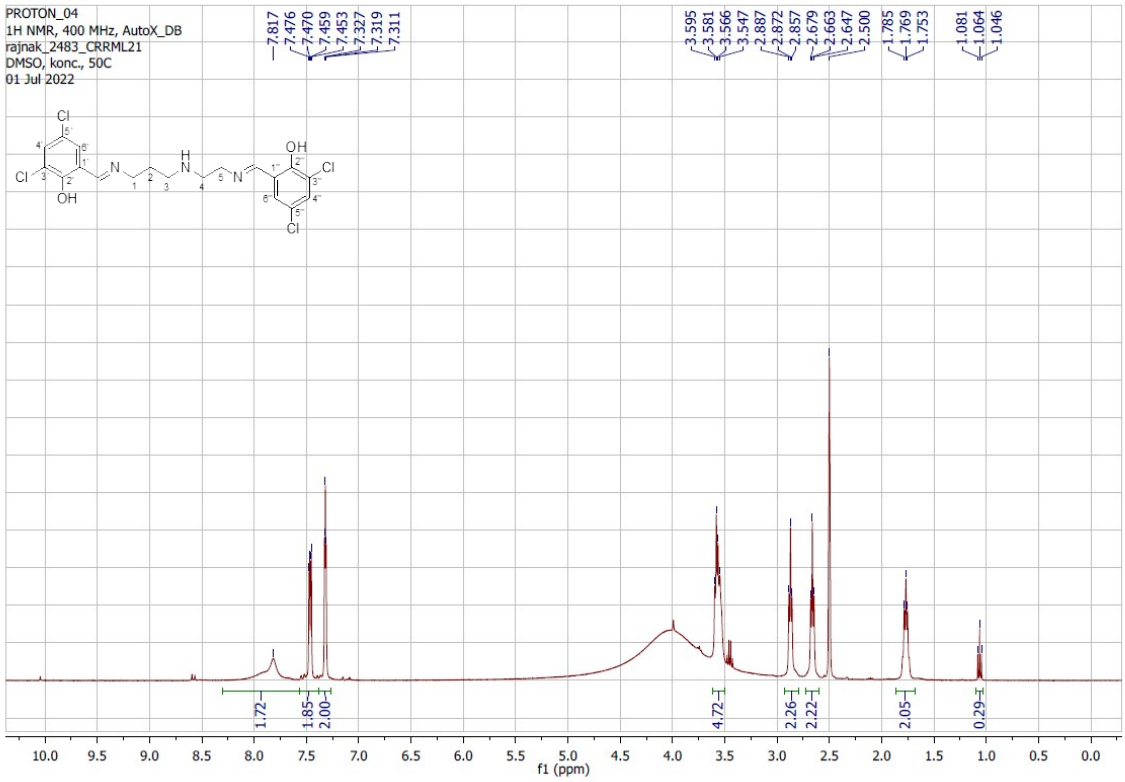

Figure S2: ^{1}H NMR spectrum for L^{im}

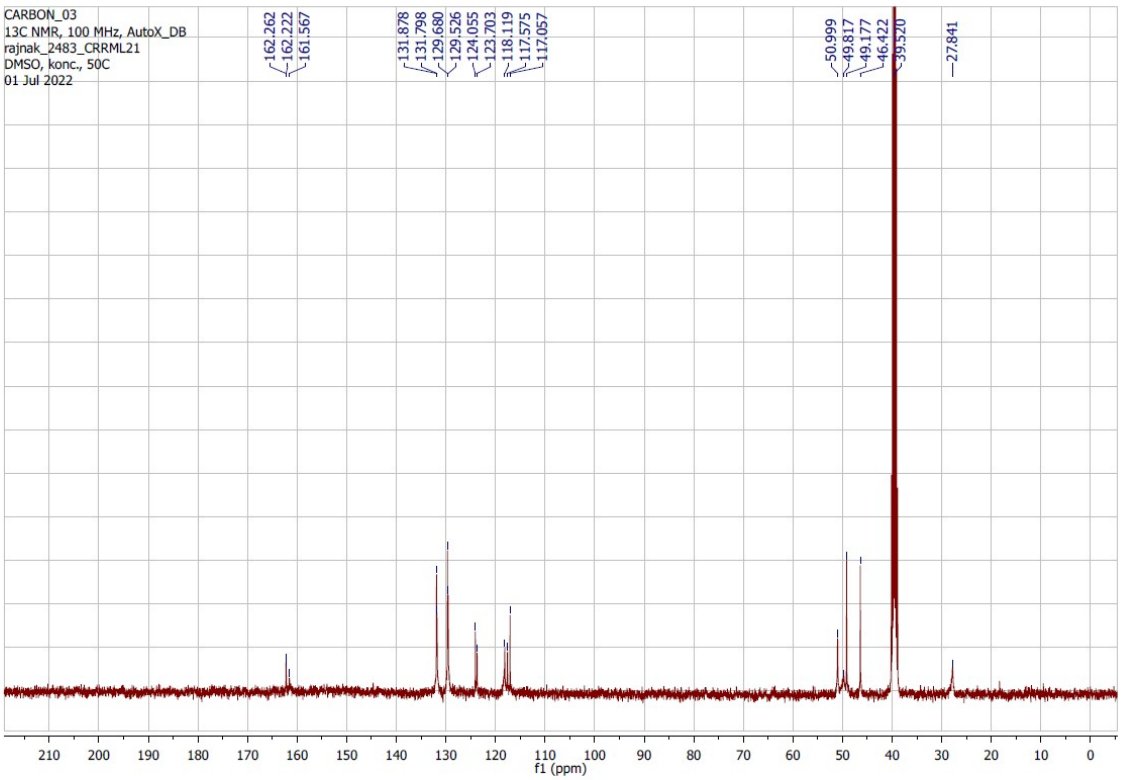

Figure S3: ^{13}C NMR spectrum for L^{am}.

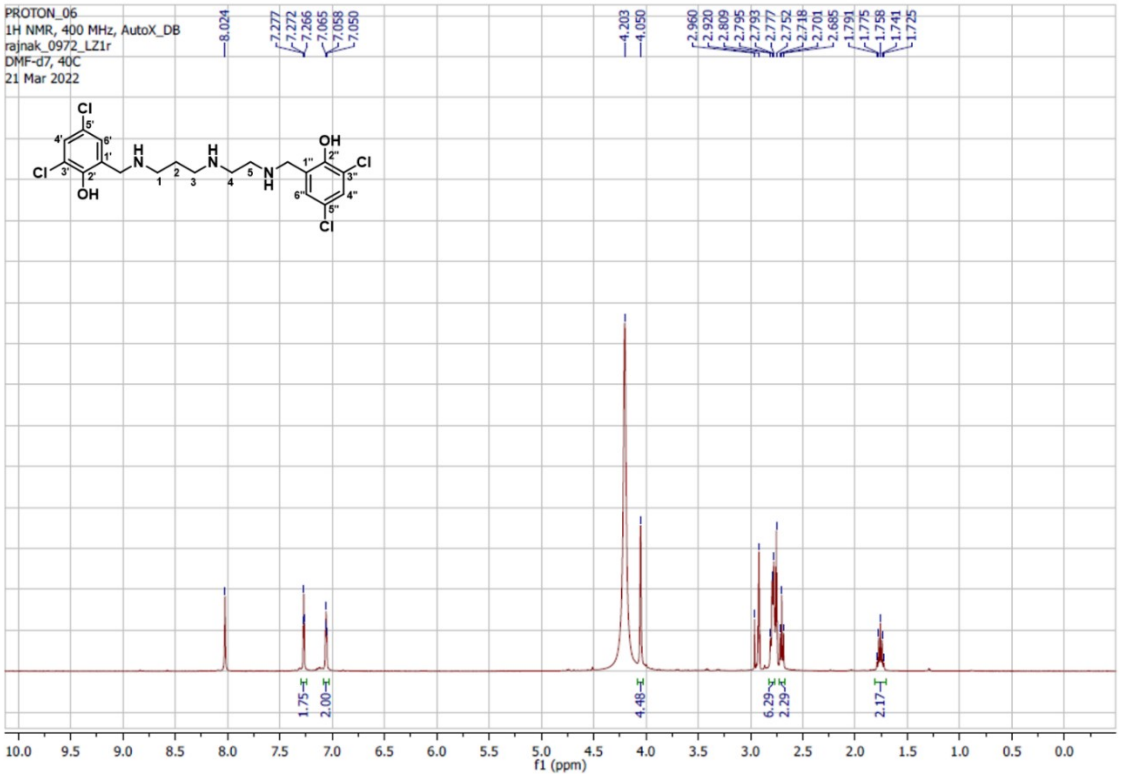

Figure S4: ^{1}H NMR spectrum for L^{am}.

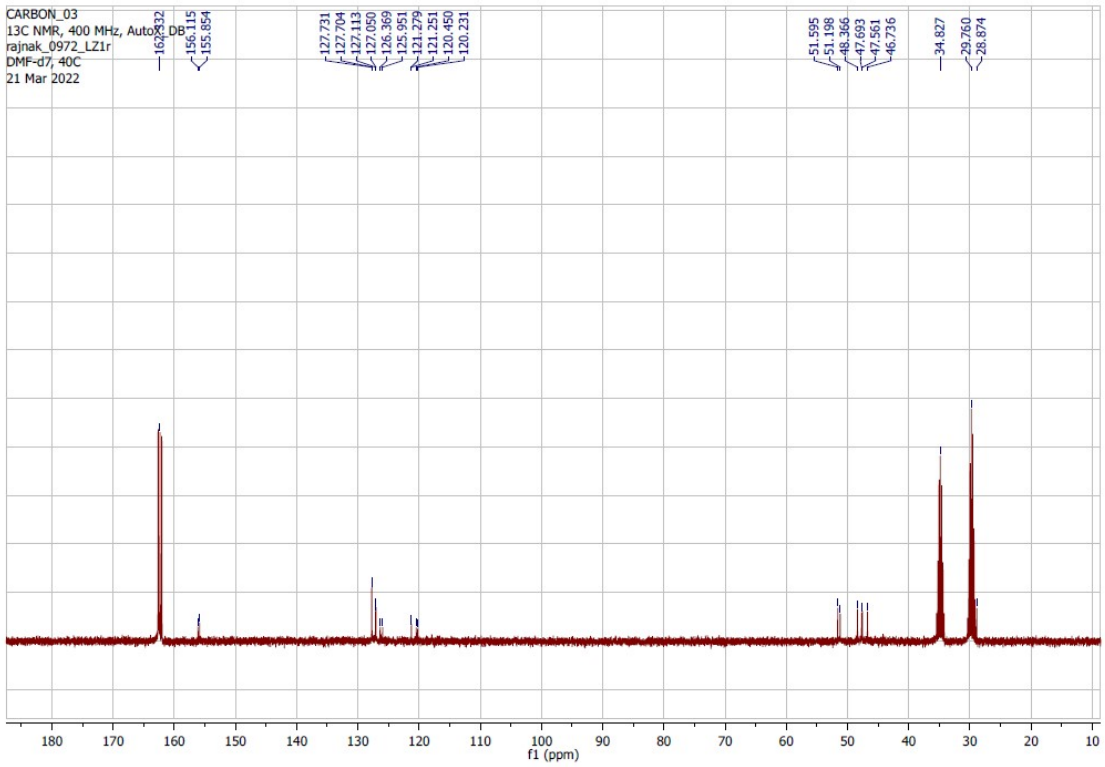

Figure S5: ^{13}C NMR spectrum for L^{am}.

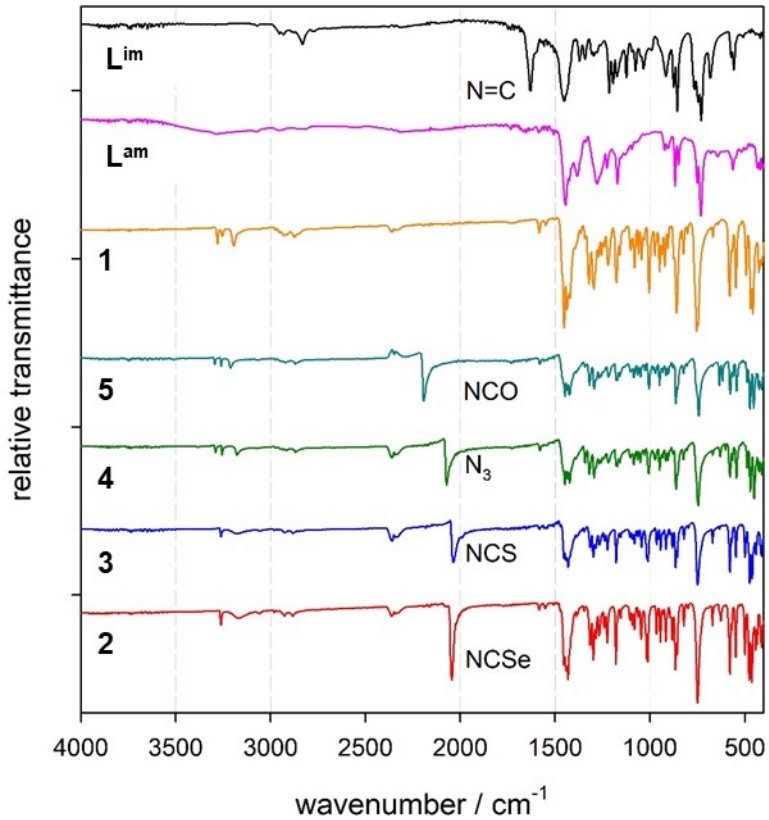

Figure S6. FTIR spectra of L^{im}, L^{am} and **1** - **5**.

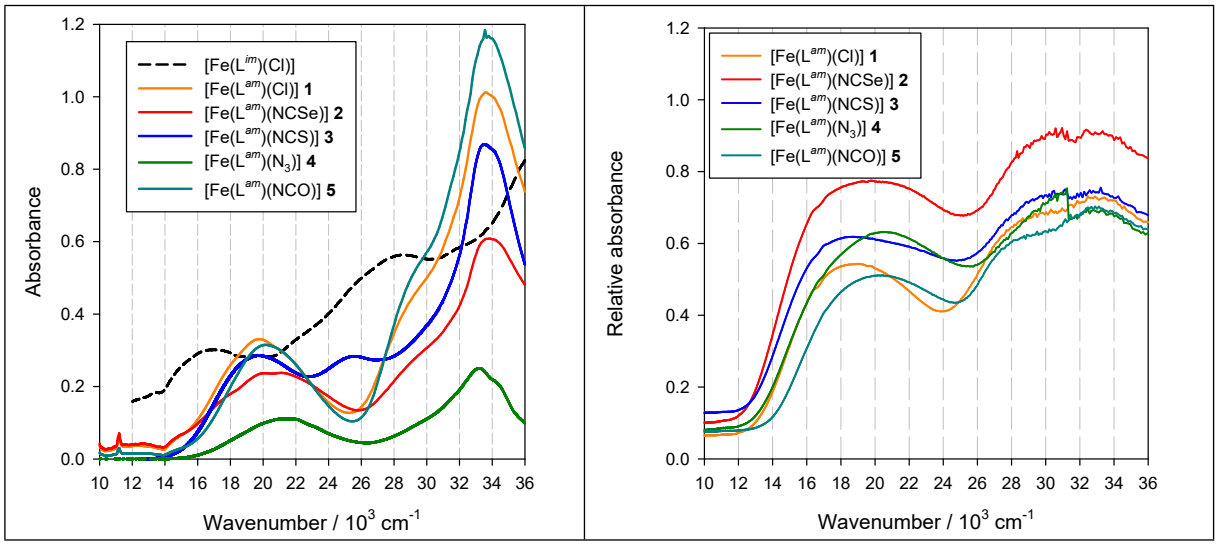

Figure S7. UV/Vis spectra of **1** - **5**. Left – in solvent. Right – in Nujol mull.
All spectra exhibit a broad d-d band referring to the spin-forbidden transition $^6A_1 \rightarrow {}^4T_1(^4G)$ at 18000 – 20000 cm^{-1} that is typical for Fe(III) complexes.
Ab initio (*in silico*) calculated sextet to quartet transitions are {15.1, 15.7, 16.5} for **1**, {15.6, 15.8, 17.9} for **2**, {15.3, 15.5, 16.9} for **3**, {14.4, 15.3, 16.0} for **4**, and {15.4, 16.1, 16.9} for **5** in units of 10^3 cm^{-1}.

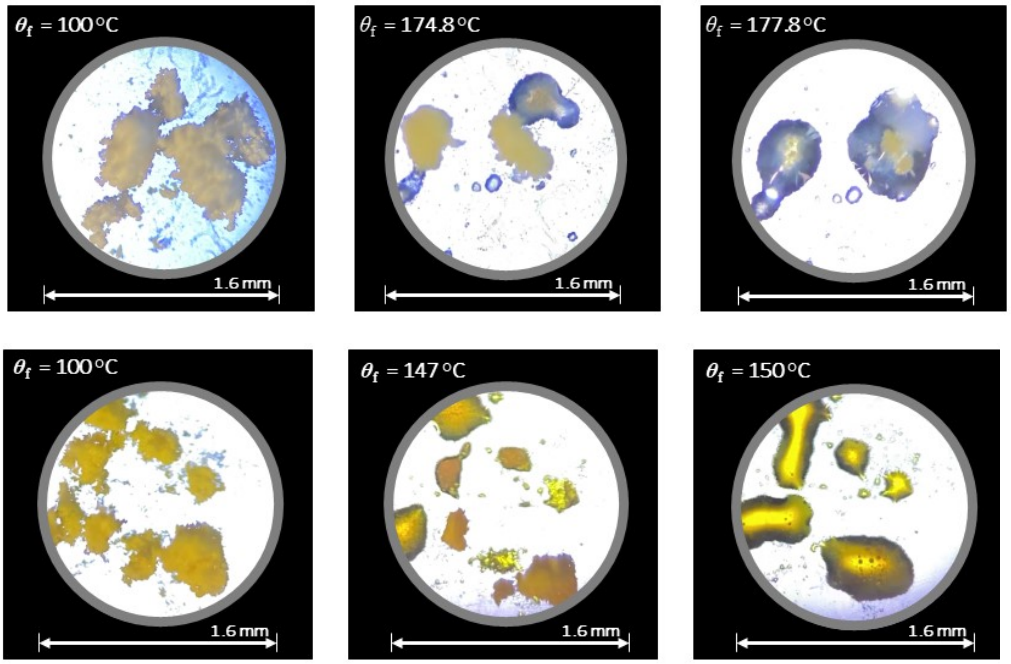

Figure S8. Melting process of powdered $\mathbf{L^{am}}$ (up) and $\mathbf{L^{im}}$ (down).

Table S1. Calculated orbital energies for $\mathbf{L^{im}}$ and $\mathbf{L^{am}}$ calculated by B3LYP/TZVP model of DFT

No	L^{im}: *E* (eV)	L^{am}: *E* (eV)
100	-9.88	-10.05
101	-9.61	-9.97
102	-9.45	-9.92
103	-9.44	-9.89
104	-9.33	-9.76
105	-9.20	-9.62
106	-9.06	-9.45
107	-8.91	-9.30
108	-8.73	-9.24
109	-8.68	-8.79
110	-8.31	-8.58
111	-8.29	-8.57
112	-7.03	-8.55
113	-7.02	-8.54
114	-6.97	-7.13
115	-6.59	-7.12
116	-6.50	-6.65
117	-6.40	-6.60
118	**-6.15 HOMO**	-6.3413
119	**-2.03 LUMO**	-6.2934
120	-1.83	**-6.23 HOMO**
121	-0.7740	**-0.88 LUMO**
122	-0.6685	-0.88
123	-0.28	-0.48
124	-0.25	-0.47
125	0.30	-0.14

Table S2. Calculated molecular properties for $\mathbf{L^{im}}$ and $\mathbf{L^{am}}$.

Property	HyperChem software		ORCA package	
	$\mathbf{L^{im}}$	$\mathbf{L^{am}}$	$\mathbf{L^{im}}$	$\mathbf{L^{am}}$
E(HOMO)	-8.744	-8.697	-6.157	-6.230
E(LUMO)	-2.08	-0.262	-2.029	-0.883
Δ*E*(HOMO-LUMO)	-6.664	-8.435	-4.128	-5.347
$I = -E$(HOMO)	8.744	8.697	6.157	6.23
$A = -E$(LUMO)	2.08	0.262	2.029	0.883
Mulliken electronegativity, χ,	5.412	4.480	4.093	3.556
Pearson hardness, η	3.332	4.217	2.064	2.674
Electrophility index $\omega = \chi^2/2\eta$	4.395	2.379	4.058	2.366

Table S3. Calculated Löwdin and Mulliken atomic charges for $\mathbf{L^{im}}$ and $\mathbf{L^{am}}$.

$\mathbf{L^{im}}$	$\mathbf{L^{im}}$: Löwdin atomic charges	$\mathbf{L^{im}}$: Mulliken atomic charges	$\mathbf{L^{am}}$	$\mathbf{L^{am}}$: Löwdin atomic charges	$\mathbf{L^{am}}$: Mulliken atomic charges
0 C	-0.408	0.142	0 C	-0.408	0.128
1 C	-0.099	-0.217	1 C	-0.117	-0.213
2 C	-0.123	0.212	2 C	-0.111	0.084
3 C	-0.221	0.072	3 C	-0.252	0.103
4 C	-0.388	0.107	4 C	-0.392	0.100
5 C	-0.138	-0.202	5 C	-0.148	-0.209
6 C	-0.168	-0.127	6 C	-0.240	-0.082
7 N	0.121	-0.161	7 N	-0.018	-0.310
8 C	-0.292	-0.132	8 C	-0.298	-0.126
9 C	-0.258	-0.129	9 C	-0.259	-0.155
10 C	-0.302	-0.110	10 C	-0.301	-0.114
11 N	-0.029	-0.306	11 N	-0.028	-0.302
12 C	-0.303	-0.060	12 C	-0.302	-0.091
13 C	-0.290	-0.103	13 C	-0.298	-0.104
14 N	0.101	-0.215	14 N	-0.019	-0.319
15 C	-0.157	-0.075	15 C	-0.239	-0.087
16 C	-0.126	0.096	16 C	-0.112	0.086
17 C	-0.237	0.152	17 C	-0.251	0.102
18 C	-0.390	0.089	18 C	-0.393	0.100
19 C	-0.137	-0.196	19 C	-0.148	-0.209
20 C	-0.405	0.168	20 C	-0.408	0.128
21 C	-0.075	-0.229	21 C	-0.117	-0.213
22 O	0.097	-0.385	22 O	0.095	-0.386
23 Cl	0.380	-0.113	23 Cl	0.375	-0.120
24 Cl	0.366	-0.107	24 Cl	0.360	-0.116
25 Cl	0.364	-0.110	25 Cl	0.360	-0.115
26 Cl	0.380	-0.111	26 Cl	0.374	-0.121
27 O	0.127	-0.316	27 O	0.096	-0.386
28 H	0.151	0.124	28 H	0.152	0.123
29 H	0.152	0.137	29 H	0.150	0.131
30 H	0.122	0.069	30 H	0.143	0.113
31 H	0.127	0.096	31 H	0.130	0.099
32 H	0.126	0.093	32 H	0.113	0.076
33 H	0.130	0.082	33 H	0.126	0.077
34 H	0.135	0.097	34 H	0.137	0.107
35 H	0.127	0.092	35 H	0.128	0.095
36 H	0.110	0.069	36 H	0.111	0.072
37 H	0.159	0.167	37 H	0.160	0.169
38 H	0.128	0.094	38 H	0.125	0.086
39 H	0.111	0.069	39 H	0.114	0.082
40 H	0.124	0.089	40 H	0.126	0.089
41 H	0.130	0.107	41 H	0.116	0.088
42 H	0.131	0.104	42 H	0.143	0.113
43 H	0.151	0.137	43 H	0.150	0.131
44 H	0.158	0.146	44 H	0.152	0.121
45 H	0.171	0.307	45 H	0.170	0.304
46 H	0.164	0.290	46 H	0.170	0.304
			47 H	0.128	0.099
			48 H	0.164	0.182
			49 H	0.164	0.183
			50 H	0.129	0.102

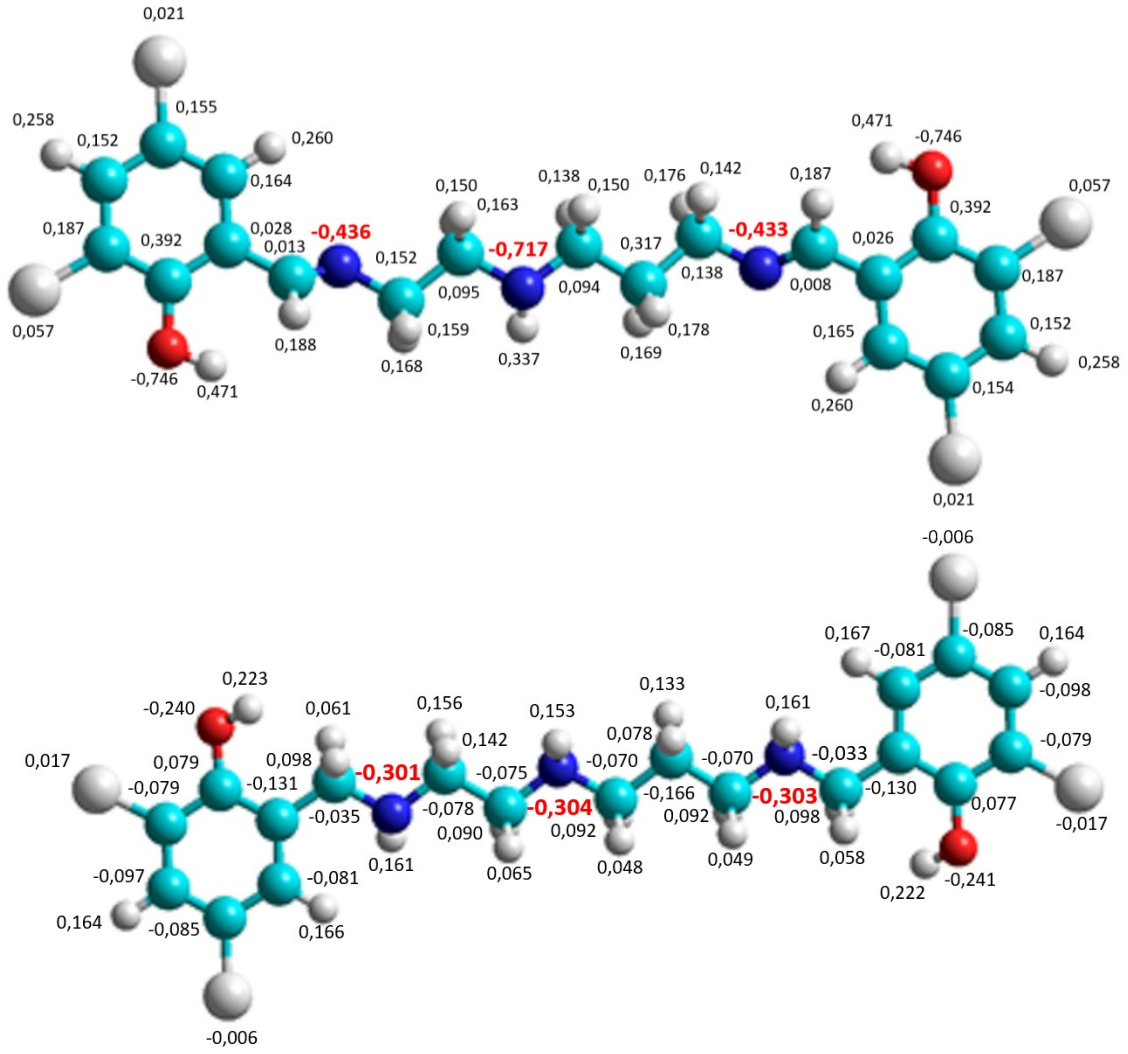

Figure S9. Atomic charges for $\mathbf{L^{im}}$ (top) and $\mathbf{L^{am}}$ (bottom).

Table S4. Crystal data and structure refinement parameters

	1	**2**	**3**	**4**	**5**
Empirical formula	$C_{19}H_{21}Cl_5FeN_3O_2$	$C_{20}H_{21}Cl_4FeN_4O_2Se$	$C_{20}H_{21}Cl_4FeN_4O_2S$	$C_{19}H_{21}Cl_4FeN_6O_2$	$C_{20}H_{21}Cl_4FeN_4O_3$
Formula weight	556.49	626.02	579.12	563.07	563.07
Temperature/K	90	100	100	100	100
Crystal system	monoclinic	orthorhombic	orthorhombic	monoclinic	monoclinic
Space group	$P2_1/c$	$P2_12_12_1$	$P2_12_12_1$	$P2_1/n$	$P2_1/n$
a/Å	10.9994(16)	7.4706(7)	7.4978(11)	14.316(2)	14.2923(8)
b/Å	8.9714(14)	11.3083(11)	11.2446(15)	9.9354(17)	10.0590(7)
c/Å	22.698(3)	27.472(2)	27.190(3)	16.168(3)	16.1597(11)
α/°	90	90	90	90	90
β/°	97.368(4)	90	90	98.476(6)	99.143(2)
γ/°	90	90	90	90	90
Volume/Å^3	2221.4(6)	2320.8(4)	2292.4(5)	2274.5(7)	2293.7(3)
Z	4	4	4	4	4
ρ_{calc} g/cm^3	1.664	1.792	1.678	1.144	1.631
μ/mm-1	1.303	2.706	1.242	1.164	1.155
F(000)	1132	1252	1180	1148.0	1152.206
Crystal size/mm^3	0.15 × 0.105 × 0.06	0.1 × 0.012 × 0.012	0.22 × 0.025 × 0.02	0.06 × 0.04 × 0.02	0.18 × 0.12 × 0.125
Radiation	0.71073	0.71073	0.71073	0.71073	0.71073
2Θ range for data collection/°	1.809 to 26.430°.	1.482 to 25.046	2.818 to 25.688	2.413 to 25.362	1.77 to 25.72
Index ranges	-13<=h<=13 -11<=k<=11 -28<=l<=20	-8<=h<=8 -10<=k<=13 -28<=l<=32	-8<=h<=9 -13<=k<=13 -30<=l<=33	-17<=h<=17 -11<=k<=11 -19<=l<=19	-17<=h<=17 -12<=k<=12 -19<=l<=19
Reflections collected	27413	23220	23408	34740	46929
Independent reflections	4552	4098	4343	4147	4382
Data/restraints/parameters	4552 / 0 / 271	4098 / 0 / 289	4343 / 0 / 290	4147 / 3 / 299	4382 / 0 / 289
Goodness-of-fit on F2	1.101	1.000	1.036	1.042	1.0480
Final R indexes [I>=2σ (I)]	R1 = 0.0439, wR2 = 0.0987	R1 = 0.0465, wR2 = 0.0901	R1 = 0.0379, wR2 = 0.0795	R1 = 0.0441, wR2 = 0.0989	R1 = 0.0275, wR2 = 0.0601
Final R indexes [all data]	R1 = 0.0599, wR2 = 0.1050	R1 = 0.0769, wR2 = 0.0992	R1 = 0.0477, wR2 = 0.0841	R1 = 0.0773, wR2 = 0.1175	R1 = 0.0398, wR2 = 0.0652
Largest diff. peak/hole / e Å^{-3}	0.809 and -0.376	0.721 and -0.758	0.374 and -0.475	0.379 and -0.619	0.4024 and -0.3621
CCDC	2154600	2154596	2154595	2154594	2154593

Hexacoordinate high-spin Fe(III) complexes composed of pentadentate amino-type ligand and pseudohalido coligands

Cyril Rajnák, Romana Mičová, Zuzana Bielková, Ján Titiš, Milan Gembický, Franz Renz, Ondřej Malina, Erika Samoľová, Jana Nováčiková and Roman Boča

Table S5. Survey of structural features for **1** through **5**.

No	Complex	Chromophore	SHAPE index[a]					Packing
			Hexagon (D6h)	PPY-6 (C5v)	OC-6 (Oh)	TPR-6 (D3h)	JPPY-5	
1	$[Fe(L^{am})(Cl)]$	$\{FeN_3O_2Cl\}$	33.120	26.769	**0.556**	14.799	31.382	dimers
2	$[Fe(L^{am})(NCSe)]$	$\{FeN_4O_2\}$	31.307	26.902	**0.388**	14.496	30.250	monomers
3	$[Fe(L^{am})(NCS)]$	$\{FeN_4O_2\}$	31.303	27.344	**0.331**	14.740	30.746	monomers
4	$[Fe(L^{am})(N)_3]$	$\{FeN_4O_2\}$	30.858	26.590	**0.456**	14.134	29.760	dimers
5	$[Fe(L^{am})(NCO)]$	$\{FeN_4O_2\}$	31.026	25.958	**0.494**	14.071	29.169	dimers

[a] PPY-6: Pentagonal pyramid, OC-6: Octahedron, TPR-6: Trigonal prism D3h, JPPY-5: Johnson pentagonal pyramid. M. Llunell, D. Casanova, J. Cirera, P. Alemany, S. Alvarez. Program SHAPE, Ver. 2.1. University of Barcelona. Note: the program assumes a spherical distribution of the ligands in ideal reference polygons or polyhedra, 2013.

Table S6. Geometric data with SHAPE index and magnetic data for **1** - **5** and similar imino compounds.

Complex	Chromophore	Spin state	Ligand form	SHAPE index	Config. isomerism	*T* / K	Ref
Amino form							
1, $[Fe(L^{am})(Cl)]$	$\{FeN_3O_2Cl\}$	HS	am	0.556	*cis* (2×O) + *fac* (3×N)	90	tw
2, $[Fe(L^{am})(NCSe)]$	$\{FeN_4O_2\}$	HS	am	0.388	*cis*	100	tw
3, $[Fe(L^{am})(NCS)]$	$\{FeN_4O_2\}$	HS	am	0.331	*cis*	100	tw
4, $[Fe(L^{am})(N)_3]$	$\{FeN_4O_2\}$	HS	am	0.456	*cis*	100	tw
5, $[Fe(L^{am})(NCO)]$	$\{FeN_4O_2\}$	HS	am	0.494	*cis*	100	tw
Imino form							
$[Fe(^5Cl\text{-}L)(Cl)]\cdot 0.25H_2O$	$\{FeN_3O_2Cl\}$	HS	im	1.055; 0.927	*cis* (2×O) + *fac* (3×N)	213	[1]
$Fe(^5Cl\text{-}L)(NCO)]$	$\{FeN_4O_2\}$	HS	im	0.830; 0.975	*cis*	293	[1]
$[Fe(^5Cl\text{-}L)(NCS)]$	$\{FeN_4O_2\}$	SCO	im	0.138	*cis*	100	[1]
$[Fe(^5Cl\text{-}L)(NCSe)]$	$\{FeN_4O_2\}$	SCO	im	0.136	*cis*	120	[1]
$Fe(^5Cl\text{-}L)(CN)]\cdot H_2O$	$\{FeN_4O_2\}$	LS	im	0.118; 0.224	*cis*	273	[1]
$[Fe(^5Br\text{-}L)(Cl)]\cdot 0.5H_2O$	$\{FeN_3O_2Cl\}$	HS	im	1.022; 0.936	*cis* (2×O) + *fac* (3×N)	90	[2]
$[Fe(^5Br\text{-}L)(NCS)]$	$\{FeN_4O_2\}$	HS	im	0.822	*cis*	213	[2]
$[Fe(^5Br\text{-}L)(N_3)]\cdot MeOH$	$\{FeN_4O_2\}$	SCO	im	1.179	*cis*	293	[2]
$[Fe(^5Br\text{-}L)(NCSe)]$	$\{FeN_4O_2\}$	SCO	im	0.152	*cis*	193	[2]
$[Fe(^{3,5}Cl\text{-}L)(Cl)]$	$\{FeN_3O_2Cl\}$	HS	im	1.074	*cis* (2×O) + *fac* (3×N)	293	[3]
$[Fe(^{3,5}Cl\text{-}L)(N_3)]$	$\{FeN_4O_2\}$	HS	im	-	-	-	[3]
$[Fe(^{3,5}Cl\text{-}L)(NCS)]$	$\{FeN_4O_2\}$	HS	im	-	-	-	[3]
$[Fe(^{3,5}Cl\text{-}L)(NCSe)]$	$\{FeN_4O_2\}$	SCO	im	0.159	*cis*	100	[3]
$[Fe(^{3,5}Br\text{-}L)(NCS)]$	$\{FeN_4O_2\}$	HS	im	-	-	-	[3]
$[Fe(^{3,5}Br\text{-}L)(N_3)]$	$\{FeN_4O_2\}$	HS	im	-	-	-	[3]
$[Fe(^{3,5}Br\text{-}L)(NCSe)]$	$\{FeN_4O_2\}$	HS	im	-	-	-	[3]

$H_2(^5Cl\text{-}L)$ = N,N'-bis(5-chloro-2-hydroxybenzylidene)-1,6-diamino-3-azahexane); $H_2(^{3,5}Cl\text{-}L)$ = N,N'-bis(3,5-di-chloro-2-hydroxybenzylidene)-1,6-diamino-3-azahexane); $H_2(^{3,5}Cl\text{-}L^{am})$ = N,N'-bis(3,5-di-chloro-2-hydroxy benzylamine)-1,6-diamino-3-azahexane).

[1] Ch. Krüger, P. Augustín, I. Nemec, Z. Trávniček, H. Oshio, R. Boča, F. Renz, Eur. *J. Inorg. Chem*, 2013, 902-915.
[2] Ch. Krüger, P. Augustín, Ľ. Dlháň, J. Pavlik, J. Moncoľ, I. Nemec, R. Boča, F. Renz, *Polyhedron*, 2015, **87**, 194-201.
[3] Rajnák, C., Titiš, J., Moncol', J., Valigura, D., Boča, R. *Inorg. Chem.,* 2020, **59**, 14871−14878.

Table S7. Bond lengths (Å) and bond angles (deg) within the coordination polyhedra.

Compounds	*d*(Fe-X)		X-Fe-Y		d_{av} (Fe-N)	d_{av} (Fe-O)
1						
	Fe1-N1	2.152(3)	Cl1-Fe1-O1	92.19(8)	2.179	1.923
	Fe1-N2	2.232(3)	Cl1-Fe1-O2	174.51(8)		
	Fe1-N3	2.154(3)	Cl1-Fe1-N1	91.27(8)		
	Fe1-O1	1.934(2)	Cl1-Fe1-N2	86.79(8)		
	Fe1-O2	1.912(3)	Cl1-Fe1-N3	85.76(8)		
	Fe1-Cl1	2.386(1)	O1-Fe1-O2	91.1(1)		
			O1-Fe1-N1	93.2(1)		
			O1-Fe1-N2	178.9(1)		
			O1-Fe1-N3	99.8(1)		
			O2-Fe1-N1	92.9(1)		
			O2-Fe1-N2	89.9(1)		
			O2-Fe1-N3	89.4(1)		
2						
	Fe1-N1	2.128(8)	O1-Fe1-O2	95.1(2)	2.16	1.919
	Fe1-N2	2.179(6)	O1-Fe1-N1	88.4(3)		
	Fe1-N3	2.205(6)	O1-Fe1-N2	91.5(2)		
	Fe1-N4	2.128(6)	O1-Fe1-N3	171.6(2)		
	Fe1-O1	1.915(5)	O1-Fe1-N4	101.0(2)		
	Fe1-O2	1.923(6)	O2-Fe1-N1	176.5(3)		
			O2-Fe1-N2	93.7(2)		
			O2-Fe1-N3	92.9(2)		
			O2-Fe1-N4	90.5(2)		
			N1-Fe1-N2	86.3(3)		
			N1-Fe1-N3	83.6(3)		
			N1-Fe1-N4	88.7(3)		
			N2-Fe1-N3	85.6(2)		
			N2-Fe1-N4	166.3(2)		
			N3-Fe1-N4	81.3(2)		
3						
	Fe1-N1	2.126(4)	O1-Fe1-O2	94.6(2)	2.154	1.919
	Fe1-N2	2.157(4)	O1-Fe1-N1	89.4(2)		
	Fe1-N3	2.215(5)	O1-Fe1-N2	91.7(2)		
	Fe1-N4	2.118(4)	O1-Fe1-N3	172.8(2)		
	Fe1-O1	1.910(4)	O1-Fe1-N4	100.4(2)		
	Fe1-O2	1.928(3)	O2-Fe1-N1	176.0(2)		
			O2-Fe1-N2	92.6(2)		
			O2-Fe1-N3	92.4(2)		
			O2-Fe1-N4	90.7(2)		
			N1-Fe1-N2	86.8(2)		
			N1-Fe1-N3	83.6(2)		
			N1-Fe1-N4	89.0(2)		
			N2-Fe1-N3	86.4(2)		
			N2-Fe1-N4	167.1(2)		
			N3-Fe1-N4	81.1(2)		
4						
	Fe1-N1	2.146(3)	O1-Fe1-O2	91.6(1)	2.144	1.929
	Fe1-N2	2.221(3)	O1-Fe1-N1	92.0(1)		
	Fe1-N3	2.167(3)	O1-Fe1-N2	176.3(1)		
	Fe1-N4	2.042(3)	O1-Fe1-N3	100.4(1)		
	Fe1-O1	1.918(3)	O1-Fe1-N4	94.5(1)		
	Fe1-O2	1.940(3)	O2-Fe1-N1	92.8(1)		
			O2-Fe1-N2	92.1(1)		
			O2-Fe1-N3	88.7(1)		

			O2-Fe1-N4	172.2(1)		
			N1-Fe1-N2	87.7(1)		
			N1-Fe1-N3	167.4(1)		
			N1-Fe1-N4	91.8(1)		
			N2-Fe1-N3	79.8(1)		
			N2-Fe1-N4	81.8(1)		
			N3-Fe1-N4	85.5(2)		
5						
	Fe1-N1	2.171(2)	O1-Fe1-O2	90.58(6)	2.144	1.9335
	Fe1-N2	2.220(2)	O1-Fe1-N1	88.76(6)		
	Fe1-N3	2.154(2)	O1-Fe1-N2	91.69(6)		
	Fe1-N4	2.031(2)	O1-Fe1-N3	93.44(6)		
	Fe1-O1	1.939(2)	O1-Fe1-N4	173.46(7)		
	Fe1-O2	1.928(1)	O2-Fe1-N1	101.29(6)		
			O2-Fe1-N2	177.51(6)		
			O2-Fe1-N3	91.46(6)		
			O2-Fe1-N4	93.53(7)		
			N1-Fe1-N2	79.80(6)		
			N1-Fe1-N3	167.05(6)		
			N1-Fe1-N4	85.44(7)		
			N2-Fe1-N3	87.38(6)		
			N2-Fe1-N4	84.30(7)		
			N3-Fe1-N4	91.55(7)		

Table S8. View on coordination polyhedra (opacity 0.65) and characteristic bond angle between central and donor atom of psedohalogene group in the amino and imino complexes.

Amino HS-route

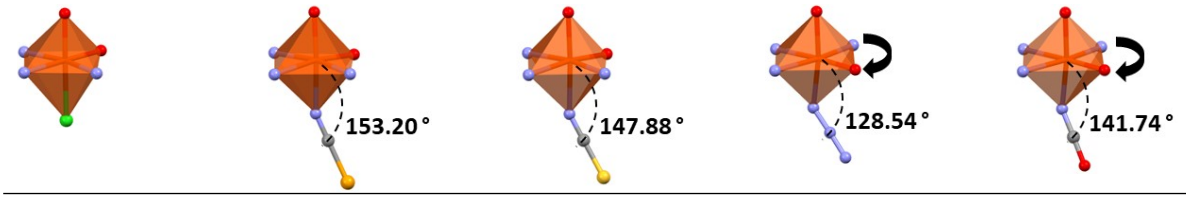

Cl (90K)	NCSe (100K)	NCS (100K)	N3 (100K)	NCO (100K)

Imino SCO-route

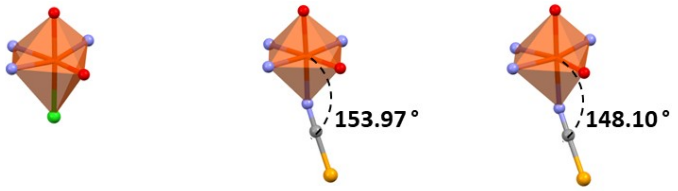

Cl (293K, HS)	NCSe (100K, LS)	NCSe (200K, HS)

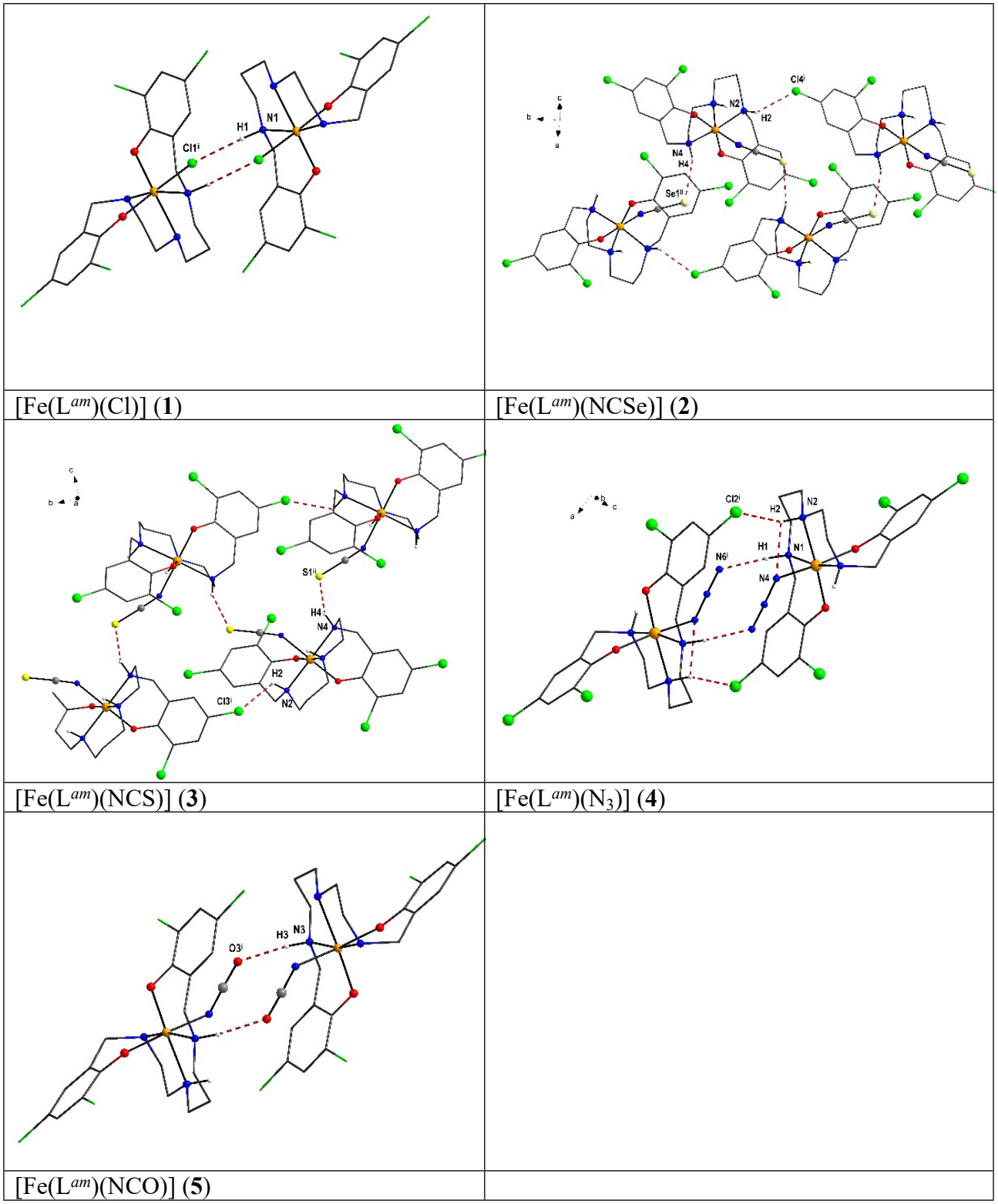

[Fe(L^{am})(Cl)] (**1**)	[Fe(L^{am})(NCSe)] (**2**)
[Fe(L^{am})(NCS)] (**3**)	[Fe(L^{am})(N$_3$)] (**4**)
[Fe(L^{am})(NCO)] (**5**)	

Figure S10. Hydrogen bonding interactions within molecular structures of **1-5**

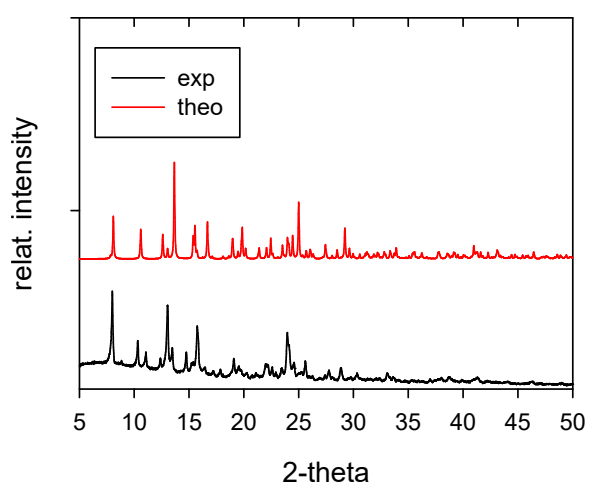

[Fe(L^{am})(Cl)] (**1**)

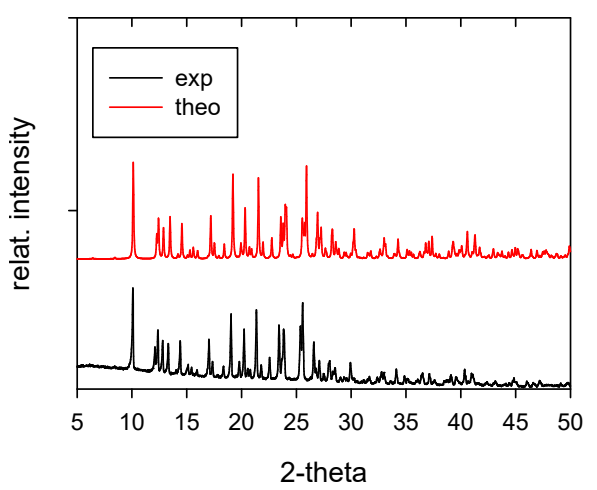

[Fe(L^{am})(NCSe)] (**2**)

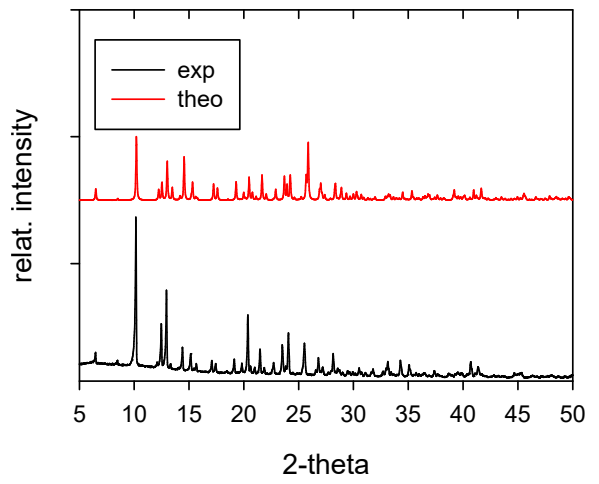

[Fe(L^{am})(NCS)] (**3**)

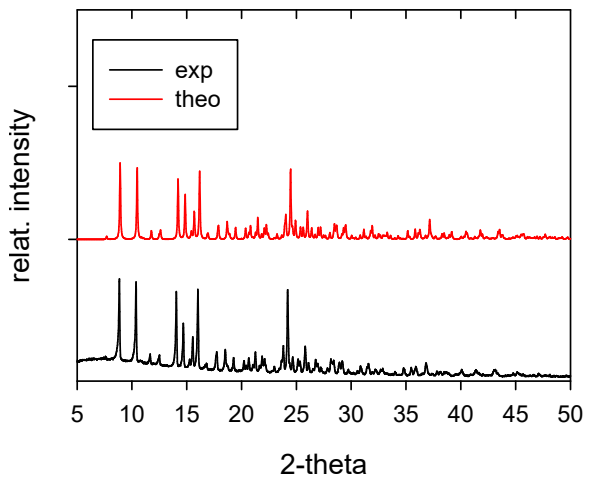

[Fe(L^{am})(N$_3$)] (**4**)

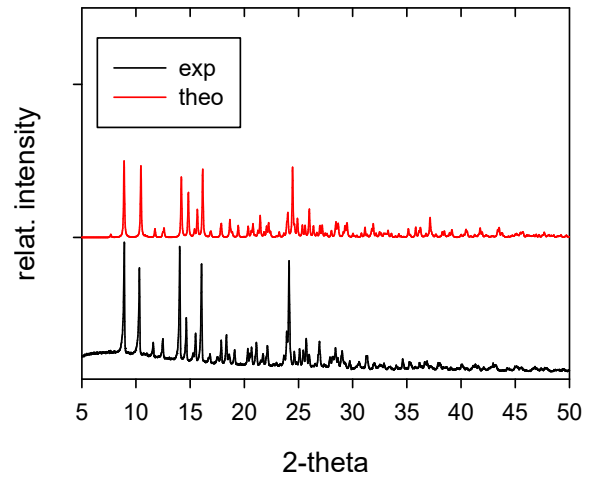

[Fe(L^{am})(NCO)] (**5**)

Figure S11. Calculated powder diffraction pattern for **1** - **5** from cif.file (red), and recorded pattern at Cu anode with λ = 1.54060 Å (black).

Table S9. Lowest sextet-to-quartet NEVPT2 transition energies and contributions to the *D*-and *E*-parameters

	1			**2**			**3**		
Root	ΔE/cm^{-1}	D_i/cm^{-1}	E_i/cm^{-1}	ΔE/cm^{-1}	D_i/cm^{-1}	E_i/cm^{-1}	ΔE/cm^{-1}	D_i/cm^{-1}	E_i/cm^{-1}
0	**15129**	**2.31**	0.00	**15622**	**-0.98**	**1.07**	**15308**	**-1.11**	**1.14**
1	**15744**	**-1.04**	**-1.05**	**15768**	**2.03**	**0.05**	**15474**	**2.19**	0.02
2	**16551**	**-0.97**	**0.98**	**16992**	**-0.94**	**-0.94**	**16880**	**-0.96**	**-0.97**
3	21298	-0.03	0.03	21836	0.00	0.01	21761	0.00	0.01
5	23179	-0.01	-0.03	22774	0.00	0.00	22519	0.01	0.00
4	26267	0.00	0.00	25665	0.00	0.00	25228	0.00	0.00
7	29389	0.00	0.00	29566	0.00	0.00	29545	0.00	0.00
6	29550	0.00	0.00	29723	0.00	0.00	29763	0.00	0.00
8	29965	0.00	0.00	29887	0.00	0.00	29856	0.00	0.00
9	32607	0.00	0.00	32091	-0.01	-0.01	32123	-0.01	-0.01
10	32673	-0.01	-0.01	32556	0.01	0.00	32511	0.01	0.00
12	33496	0.00	0.00	33566	0.00	0.00	33520	0.00	0.00
11	35040	-0.01	0.01	35403	0.00	0.00	35463	0.01	0.00
13	35681	0.00	0.00	35600	0.00	0.00	35550	0.00	0.00
14	**43202**	**-0.69**	**0.53**	**42534**	**-0.71**	**-0.72**	**42707**	**-0.72**	**-0.70**
15	**44059**	**-0.68**	**-0.51**	**44578**	**1.25**	0.02	**44645**	**1.25**	0.03
16	**44905**	**1.31**	0.00	**44946**	**-0.60**	**0.63**	**45116**	**-0.59**	**0.61**
17	47264	0.00	0.00	46514	0.00	0.00	46276	0.00	0.00
18	51920	-0.01	0.01	51783	-0.01	0.01	51866	-0.01	0.01
19	52031	0.02	0.00	52087	0.02	0.00	52191	0.03	0.00
21	52671	-0.01	-0.01	52740	-0.01	-0.01	52866	-0.02	0.00
20	55075	0.00	0.00	55099	0.00	0.00	55576	0.00	0.00
22	59332	0.00	0.00	59295	0.00	0.00	59365	0.00	0.00
23	60962	0.00	0.00	60015	0.00	0.00	60004	0.00	0.00

	4			**5**		
Root	ΔE/cm^{-1}	D_i/cm^{-1}	E_i/cm^{-1}	ΔE/cm^{-1}	D_i/cm^{-1}	E_i/cm^{-1}
0	**14400**	**2.44**	0.00	**15368**	**-1.03**	**1.06**
1	**15298**	**-1.07**	**-1.06**	**16058**	**1.78**	**-0.05**
2	**16019**	**-1.01**	**1.00**	**16865**	**-0.71**	**-0.88**
3	20362	-0.04	0.03	21638	0.02	0.00
5	23204	-0.02	-0.03	22906	-0.02	0.01
4	25867	0.00	0.00	25966	0.00	0.00
7	29111	0.00	0.00	29430	0.00	0.00
6	29319	0.00	0.00	29546	0.00	0.00
8	29806	0.00	0.00	29832	0.00	0.00
9	32470	0.00	0.00	32256	-0.01	-0.01
10	32485	-0.01	-0.01	32430	0.01	0.00
12	33226	0.00	0.00	33477	0.00	0.00
11	34719	-0.01	0.01	35220	0.00	0.00
13	35484	0.00	0.00	35495	0.00	0.00
14	**42997**	**-0.70**	**0.45**	**42901**	**-0.71**	**-0.71**
15	**44124**	**-0.68**	**-0.43**	**44342**	**1.28**	0.03
16	**44910**	**1.29**	0.00	**44694**	**-0.59**	**0.63**
17	46989	0.00	0.00	46311	0.00	0.00
18	51799	-0.01	0.01	51693	-0.01	0.00
19	51835	0.02	0.00	52012	0.01	0.00
21	52554	0.01	-0.01	52393	0.00	0.00
20	55174	0.00	0.00	54721	0.00	0.00

22	58764	0.00	0.00	59060	0.00	0.00
23	61344	0.00	0.00	59950	0.00	0.00